DOI:10.1021/jf103309b

JOURNAL OF AGRICULTURAL AND FOOD CHEMISTRY
ARTICLE

Isobaric Labeling Approach to the Tracking and Relative Quantitation of Peptide Damage at the Primary Structural Level

Anita J. Grosvenor,[†] James D. Morton,[§] and Jolon M. Dyer*,[†]

[†]Protein Quality and Function, Lincoln Research Centre, AgResearch, New Zealand, and
[§]Department of Wine, Food and Molecular Biosciences, Lincoln University, New Zealand

Protein oxidative damage lies behind skin and hair degradation and the deterioration of protein-based products, such as wool and meat, in addition to a range of serious health problems. Effective strategies to ameliorate degenerative processes require detailed fundamental knowledge of the chemistry at the molecular level, including specific residue-level products and their relative abundance. This paper presents a new means of tracking damage-induced side-chain modification in peptides using a novel application for isobaric label quantification. Following exposure to heat and UVA and UVB irradiation, tryptophan and tyrosine damage products in synthetic peptides were characterized and tracked using ESI-MS/MS and iTRAQ labeling-based relative quantification. An in-depth degradation profile of these peptides was generated, enabling the formation of even low-abundance single-residue-level modifications to be sensitively monitored. The development of this novel approach to profiling and tracking residue-level protein damage offers significant potential for application in the development and validation of protein protection treatments.

KEYWORDS: Protein damage; iTRAQ quantitation; oxidation; damage tracking; mass spectrometry

INTRODUCTION

The degradation of amino acid residues within proteins is a critical concern across a broad spectrum of substrates. Protein damage is an important component in the development of a range of diseases, such as cataracts (*1*), atherosclerosis (*2*), and aging (*3*) and in the processing- and aging-related deterioration of protein-based materials such as hair (*4*), skin (*5*), wool (*6*), silk (*7*), milk (*8*), and meat (*9*). Accordingly, many of the residue modifications associated with protein damage have been qualitatively characterized using techniques such as Raman spectroscopy (*10*) and mass spectrometry (MS) (*11*). Nevertheless, currently holistic assays [such as the detection of carbonyl groups (*12*, *13*), assays for specific oxidation products (*14*, *15*), or physical changes in the substrate (*16*, *17*)], which suffer from a lack of specificity and an inability to localize damage to specific proteins (*18*), remain the predominant methods for quantifying protein damage. Residue-level changes, which can impart significant changes in protein functionality, can be induced by diverse insults such as exposure to heat (*19*), light (*20*), cellular sensitizers (*3*), oxidants (*21*), and acids (*22*) and are therefore important in both intra- and extracellular systems. The impact of residue-level damage on biological and product systems and the expanding field of redox proteomics demand accurate and sensitive tools for profiling and tracking damage at the molecular level.

We present here a novel utilization of isobaric labeling for tracking protein damage, which utilizes the accuracy of MS for qualitative and quantitative characterization of residue damage. Isobaric labeling has been developed for the mass spectrometric comparative quantitation of proteins (or cellular post-translational modifications such as phosphorylation), via the labeling and pooling of peptides or proteins with isomer-balanced chemicals so that differentially labeled peptides have the same mass and chemical composition. Isomer differences are revealed during tandem mass spectrometry (MS/MS) fragmentation, allowing relative quantitation between samples (*23*). The primary isobaric labeling system currently employed is iTRAQ labeling (*24*), which enables labeling of up to eight samples with isobaric tags; other systems reported include tandem mass tags (TMT) (*25*) and isobaric peptide termini labeling (IPTL) (*26*). In shotgun proteomics (*27*), the relative abundance of several peptides, as determined by the peak areas of the iTRAQ reporter ions, is used to determine the abundance of their parent proteins (*28*). Protein quantitation thus uses quantitative data from several peptides to make an estimation of protein abundance. We describe a novel additional application for stable isotope labeling: the quantitation of low-abundance degradative modifications in individual peptides. This approach requires sufficiently accurate quantitative information to be obtained from a single peptide variant to allow observation of the differences between samples, necessitating a modified approach to quantitative analysis. We have evaluated the ability of isobaric peptide labeling to deliver sufficiently accurate quantitation of specific peptide modifications.

In contrast to holistic approaches to protein damage quantitation, this approach provides information on the specific chemistry of the residue modification, its location in a specific residue within a peptide sequence, and its rate of formation. This enables the generation of detailed degradation profiles, which may provide information on the chemistry of modification, including the formative mechanisms and pathways of formation.

*Corresponding author (e-mail jolon.dyer@agresearch.co.nz).

 Published on Web 11/18/2010

This paper describes the application of isobaric quantification to tracking the low-abundance residue-level damage inflicted on short synthetic peptides exposed to high temperatures and UVA and UVB irradiation.

MATERIALS AND METHODS

Materials. HPLC-grade ethanol was obtained from Fisher Scientific (Loughborough, U.K.); ChromAR LC-grade water from Mallinckrodt Chemicals; LC-grade acetonitrile from J. T. Baker (Phillipsburg, NJ); and Univar formic acid from Ajax Finechem (Auckland, New Zealand). NanoES spray capillaries were obtained from Proxeon Biosystems (Odense, Denmark). Synthetic peptides Leu-Leu-Tyr-Leu-Arg-OH (LLYLR) and Leu-Leu-Trp-Leu-Arg-OH (LLWLR) were obtained as lyophilized hydrochloride powders from The Biopeptide Co.mpany (San Diego, CA). MS analysis confirmed the presence of these peptides, along with the truncations LLW and LLY. iTRAQ reagents were obtained from Applied Biosystems (Scoresby, Australia).

Peptide Exposure. Aqueous tyrosine- and tryptophan-containing peptide solutions were prepared by the addition of HPLC-grade water to the lyophilized powders at 2 mg/mL, pH 3.5 (not adjusted). Samples exposed to UVA or UVB were transferred to UV-transparent quartz test tubes sealed with UV-transparent polyethylene film at an approximate sample depth of 1 cm and placed in a photoirradiator (LZC4-14, LuzChem, Ontario, Canada) with UVA or UVB LZC narrow-bandwidth lamps. The spectral distribution peaks ranged over approximately 281−360 nm for the UVB and 316−400 nm for the UVA lamps, with a maximum intensity of 52670 mW m^{-2} nm^{-1} (*29*, *30*). Irradiation was performed over 12 h (UVB) and 24 h (UVA). Samples exposed to heat were transferred to sealed narrow glass tubes and heated at 90 °C over 192 h. Sample aliquots were removed and stored in the dark at −85 °C at zero time and at various time points throughout the treatment.

Isobaric Labeling. Sample aliquots of 40 μL were reduced to dryness at 30 °C in a Centrivap centrifugal concentrator (Labconco, Kansas City, MO) and reconstituted in 30 μL of 0.5 M triethylammonium bicarbonate, pH 8.5. Labeling with iTRAQ reagents was performed essentially as per the manufacturer's protocol: 70 μL of MS-grade ethanol was added to each iTRAQ reagent vial (114, 115, 116, and 117), combined, and added to the 30 μL sample aliquot. Aliquots from each sample were checked by MS for complete labeling, after which the samples were pooled. Following labeling, three aliquots from each sample were desalted and purified by 5:7 dilution in water before processing through C18 StageTips (Proxeon Biosystems) and elution into 50% acetonitrile−1% formic acid.

Mass Spectrometry. Electrospray ionization (ESI) MS analysis was performed on a tandem quadrupole time-of-flight (Qq-TOF) mass spectrometer (QSTAR Pulsar-i; Applied Biosystems, Foster City, CA) utilizing direct infusion nanospray delivery of aqueous samples. Collision-induced dissociation (CID) utilized nitrogen gas, with collision energies manually adjusted for optimal fragmentation. The QSTAR was operated with Analyst QS service pack 7 software (Applied Biosystems). Sequencing was performed manually through analysis of overlapping fragment ion series. Duplicate MS scans were taken for each subsample from m/z 200 to 900. MS/MS was performed on randomized order peak−lists of masses of modified and unmodified peptides to generate iTRAQ reporter ion data. Pooled iTRAQ samples were used throughout these experiments.

Data Analysis. A combination of MS and MS/MS data was used to track the formation of modifications in the model peptides: the MS/MS data revealed the relative abundance of any given peptide between samples (via the peak areas of reporter ions), allowing the change in the abundance of that peptide over the time course to be observed. In MS, the peak areas corresponding to the m/z of peptides labeled only at the N-terminus were recorded, allowing estimates of the relative abundance of each peptide species compared to the others present at each time point. iTRAQ labels were not detected on tyrosine residues within these peptides. The interspecies comparisons were based on an assumption that modified peptides can be expected to ionize similarly in MS, due to their possession of chemical and physical characteristics very similar to those of their parent peptides (*31*, *32*). These estimations of species abundance were used to provide species-specific weighting factors for the iTRAQ reporter ion data. These interspecies comparisons (MS) are less reliable than iTRAQ-generated intraspecies quantitation (MS/MS), but nevertheless provide a valuable opportunity for estimating the relative abundances of the degraded species. This generated a peptide degradation profile for the samples over the time course, with increases or decreases in peptide abundance evident from MS/MS data, and the relative abundance of particular species evident from the MS data. For ease of presentation, relative abundance scales have been arbitrarily adjusted so that at zero time, the unmodified peptide has a relative abundance of 1.0 (*33*).

Table 1. Tryptophan- and Tyrosine-Derived Modifications Monitored in Synthetic Peptides Using Isobaric-Labeling-Based Product Tracking

mass change (Da)	modification	proposed product(s)	numbering for figures
+16	W + O	hydroxytryptophan	product 1
+32	W + 2O	dihydroxytryptophan/ *N*-formylkynurenine	product 2
+14	W + O − C	kynurenine	product 3
+48	W + 3O	hydroxyformylkynurenine	product 4
+64	W + 4O	dihydroxyformylkynurenine	product 5
+20	W + 2O − C	hydroxykynurenine	product 6
+30	W + 2O − 2H	tryptophandione	product 7
+28	W + 2O − 4H	β-unsaturated tryptophandione	product 8
+44	W + 3O − 4H	hydroxybistryptophandione	product 9
+12	W + C	tetrahydro-β-carboline	product 10
+45	W + N + 2O − H	nitrotryptophan	product 11
+16	Y + O	diphenylalanine (dopa)	product 12
+32	Y + 2O	triphenylalanine (topa)	product 13
+14	Y + O − 2H	dopa-quinone	product 14
+30	Y + 2O − 2H	topa-quinone	product 15
+45	Y + N + 2O − H	nitrotyrosine	product 16

RESULTS AND DISCUSSION

Modifications to tyrosine and tryptophan residues previously observed and characterized in model peptides (*34*) were identified by their m/z ratios and targeted in MS/MS to generate iTRAQ reporter ion ratios. Monitored tryptophan and tyrosine degradation products are represented in **Table 1** (*34*, *35*). The structures are given in **Figure 1**.

The formation of these 16 modified products (with a wide range of relative abundances) in 4 peptides was tracked following exposure to UVA, UVB, and heat. Refer to **Figure 1** for the structures of these products. MS scans provided information on which modifications within parent peptides were most abundant, whereas MS/MS fragmentation released isobaric reporter ions that demonstrated the changes in abundance (rate of formation/degradation) of individual modifications over exposure. An MS scan of a pooled, treated sample is shown in **Figure 2**, providing an example of the peak area differences that can be used to estimate the species-to-species relative abundance and normalize isobaric quantitative information. The inset demonstrates the degradation of LLW during heat treatment, as represented by decreases in the relative abundance of the respective iTRAQ reporter ions. Isobaric labeling enables much more accurate quantification than is possible using MS peak area analysis alone; as samples are pooled, experimental variation is greatly reduced, which allows the comparison of stoichiometric reporter ions within a single MS/MS scan (*23*). By combining this information with MS-derived information regarding the contribution of the specific modification to the total ion count, a degradation product profile can be visualized, showing the change in abundance of multiple degradation products over the treatment. The depletion of parent peptides may also be visualized using isobaric reporter ion ratios (**Figure 3**). Depletion data provide a measure of the extent of degradation within a sample.

Figure 3 demonstrates the depletion of the peptide, LLW, following exposure to UVB, UVA, and hydrothermal insult.

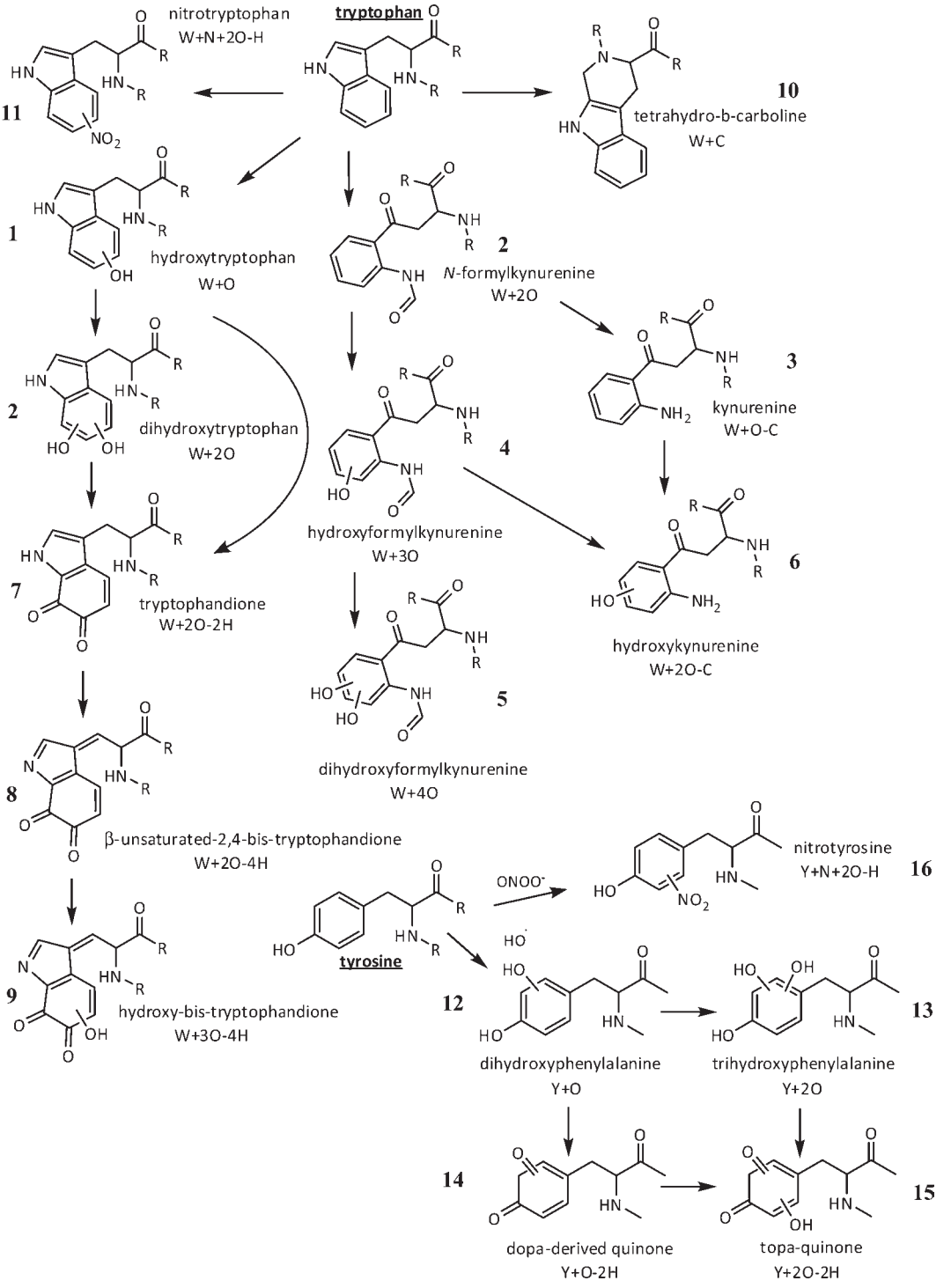

Figure 1. Derivatives of tryptophan and tyrosine, with modification and product number.

The observed decay in this peptide and in others was tracked using isobaric reporter ion MS/MS and MS scan data. The precision of measurement is indicated by small standard errors of the mean (error bars), while the rapid degradation observed after UVB irradiation is consistent with the susceptibility of tryptophan residues to the reactive oxygen species generated by short-wavelength irradiation (*36*). The profiles for the degradation products of four peptides exposed to three damage protocols are represented in **Figures 4**−**6**.

This approach allowed the progression of multiple peptide products to be sensitively monitored and subtle differences between samples to be identified. Up to 11 tryptophan residue modifications and 5 tyrosine residue modifications [see Grosvenor et al. (*34*) for a description of characterization and formation] were observed to be formed from the synthetic peptides LLWLR, LLW, LLYLR, and LLY after irradiative or hydrothermal insult. The contribution of each modified species to the degradation of each peptide can be visualized by its relative abundance, whereas its rate of formation can be seen by its changes in abundance over time.

Tracking enabled the subtle differentiation of degradation patterns between internalized or C-terminal tryptophan residues (**Figures 4**−**6**), with secondary products, such as W + 2O − 2H, W + 2O − 4H, and W + C (products 8, 9, and 10) in tryptophan and Y + 2O − 2H (product 15) in tyrosine, seen to contribute

more significantly toward degradation profiles in peptides with terminal aromatic residues than in those with internalized residues, compared to primary products such as W + O, W + 2O, and W + O − C (products 1, 2 and 3) in tryptophan and W + O (product 12) in tyrosine. Note that residue location within peptides is expected to affect reactivity, with factors such as steric hindrance and electron density affecting reaction with nucleophiles (*37*, *38*).

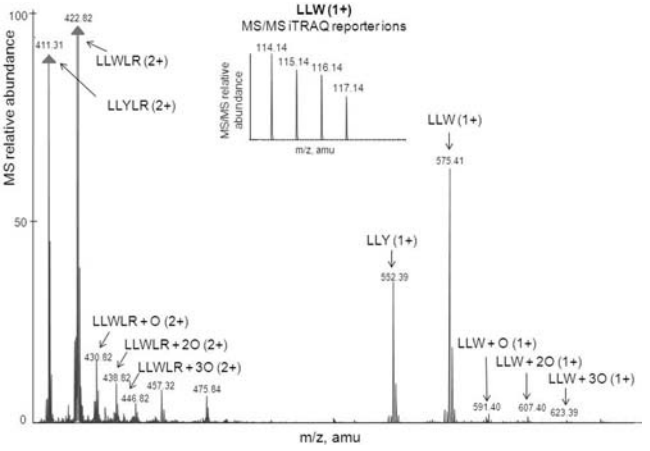

Figure 2. Portion of an MS scan of a pooled iTRAQ labeled mixture of heat-treated and untreated peptides LLWLR, LLW, LLYLR, and LLY. MS relative abundance is indicated by an arbitrary scale. (Inset) MS/MS data showing the detection of iTRAQ reporter ions for singly charged LLW. Reporter 114 corresponded to untreated sample, 115 to 48 h heat-treated sample, 116 to 96 h heat-treated sample, and 117 to 192 h heat-treated sample.

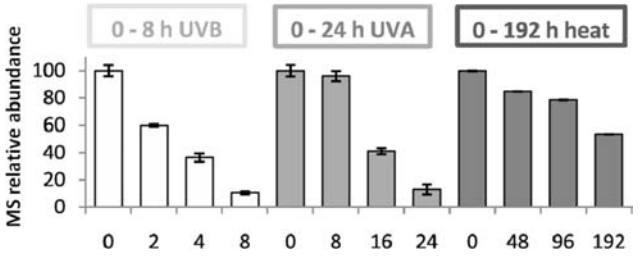

Figure 3. Depletion of parent peptide, LLW, after exposure to UVB, UVA, and 90 °C heat. Changes in abundance were determined by iTRAQ reporter ion abundance. MS relative abundance represents the peak area relative to unmodified LLW at 0 h, defined as 100. Error bars represent ± SEM (note: small error bars present on the 0−192 h heat columns may not resolve well).

The generally less regular patterns of formation (higher error, inconsistent trend) observed for tyrosine degradation products compared to tryptophan products are consistent with the lower susceptibility of tyrosine residues than tryptophan residues to direct irradiation and to the oxidative modification during irradiation and heating (*37*, *39*). Tracking revealed the already relatively high levels of some oxidative modifications prior to some treatments (such as Y + O), allowing this to be compared to their abundance post-treatment. Oxidative modifications such as this that were observed in untreated samples are attributed to in-solution sample oxidation during storage.

The formation of even low-abundance residue modifications was evident (see **Figure 5**, products 4−11 in LLWLR). The sensitivity of an isobaric MS approach to tracking protein damage is indicated by the precision of measurement of even low-abundance compounds (compare the low abundance of products 4−11 in **Figure 5** with the relatively low levels of error presented in **Table 2**). **Figure 5** demonstrates that, compared to hydroxytryptophan residue formation (W + O, product 1), the relative abundance of products 4−11 is very low, especially when derived from LLWLR. **Table 2** demonstrates the successful tracking of the increasing abundance of these minor LLWLR derivatives (products 4−11) over UVB exposure. Associated errors tend to be larger relative to the measurement when products are detected at low abundance, as would be expected, but still permit the observation of their formation.

Our novel application of isobaric labeling allowed the mass spectrometric tracking of single peptide-bound tryptophan and tyrosine modification, facilitating in-depth degradation profiling. This represents a significant variation from the conventional usage of isobaric labeling of multiple peptides to generate quantitative information on one protein. Our new approach yielded information on the degradation product species formed, their contribution to the degradation products pool, and their formation during the course of insult. Low variation between replicates demonstrated the suitability of the approach for precisely tracking the formation of even very low abundance modified

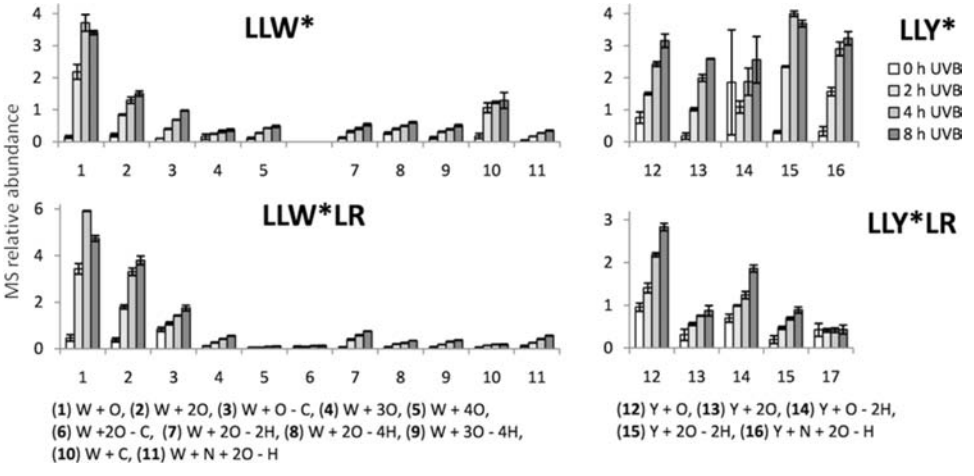

Figure 4. Tryptophan- and tyrosine-derived modifications in LLW*, LLW*LR, LLY*, and LLY*LR following UVB exposure. Changes in the abundance of modified species were determined by isobaric reporter ion abundance, whereas the relative abundance of the modified peptides was determined by MS scan. MS relative abundance represents the peak area relative to the unmodified peptides, LLW, LLWLR, LLY, or LLYLR, at 0 h, defined as 100. Error bars represent ± SEM.

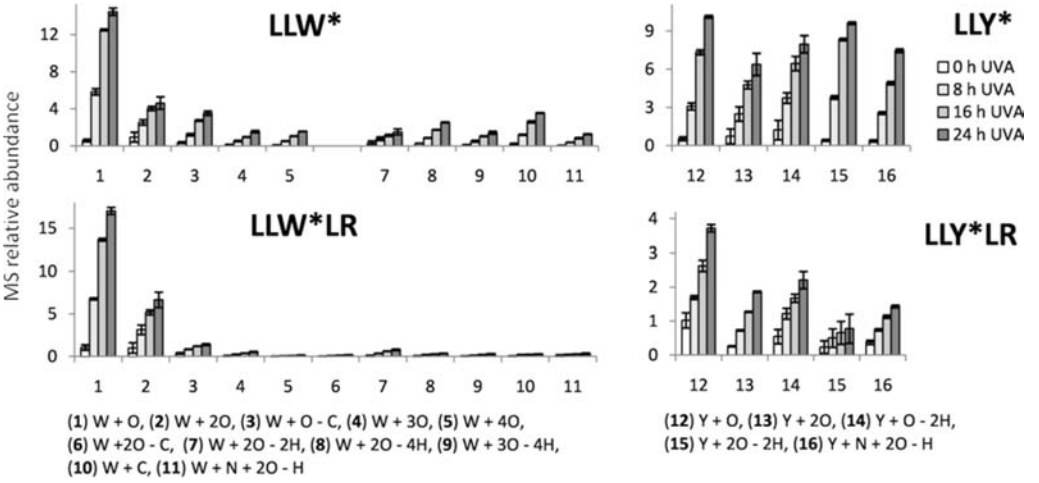

Figure 5. Tryptophan- and tyrosine-derived modifications in LLW*, LLW*LR, LLY*, and LLY*LR following UVA exposure. Changes in the abundance of modified species were determined by isobaric reporter ion abundance, whereas the relative abundance of the modified peptides was determined by MS scan. MS relative abundance represents the peak area relative to the unmodified peptides, LLW, LLWLR, LLY, or LLYLR, at 0 h, defined as 100. Error bars represent ± SEM.

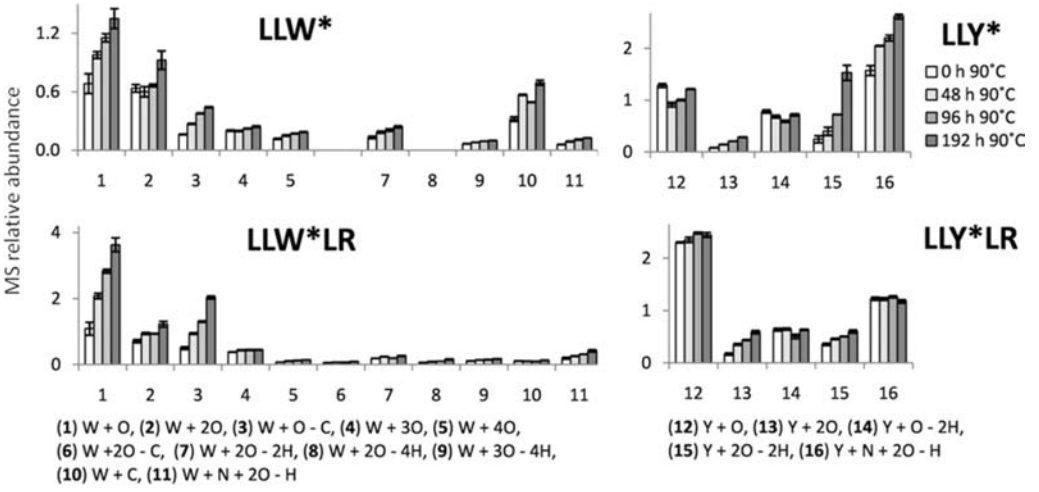

Figure 6. Tryptophan-derived modifications in LLW*, LLW*LR, LLY*, and LLY*LR following hydrothermal insult at 90 °C. Changes in the abundance of modified species were determined by isobaric reporter ion abundance, whereas the relative abundance of the modified peptides was determined by MS scan. MS relative abundance represents the peak area relative to the unmodified peptides, LLW, LLWLR, LLY, or LLYLR, at 0 h, defined as 100. Error bars represent ± SEM.

Table 2. Abundance of Selected Tryptophan Product Degradation in LLWLR after Exposure to UVB Radiation Relative to Unmodified LLWLR at 0 h (Defined as 100)[a]

LLWLR	0 h UVB	2 h UVB	4 h UVB	8 h UVB
tryptophan [W]	100 (8%)	71 (3%)	50 (4%)	25 (28%)
product 1 [+ O]	0.47 (29%)	3.43 (7%)	5.92 (0.3%)	4.74 (3%)
product 2 [+ 2O]	0.38 (23%)	1.80 (5%)	3.31 (5%)	3.80 (5%)
product 3 [+ O − C]	0.84 (11%)	1.09 (6%)	1.43 (1%)	1.75 (7%)
product 4 [+ 3O]	0.12 (10%)	0.27 (7%)	0.43 (2%)	0.56 (2%)
product 5 [+ 4O]	0.05 (44%)	0.06 (7%)	0.09 (10%)	0.11 (10%)
product 6 [+ 2O − C]	0.09 (37%)	0.09 (14%)	0.12 (10%)	0.12 (19%)
product 7 [+ 2O − 2H]	0.08 (10%)	0.40 (8%)	0.59 (4%)	0.76 (1%)
product 8 [+ 2O − 4H]	0.08 (18%)	0.20 (3%)	0.25 (7%)	0.35 (1%)
product 9 [+ 3O − 4H]	0.08 (23%)	0.18 (2%)	0.31 (5%)	0.37 (4%)
product 10 [+ C]	0.05 (51%)	0.15 (2%)	0.19 (3%)	0.19 (10%)
product 11 [+ N + 2O − H]	0.12 (27%)	0.26 (3%)	0.42 (4%)	0.57 (2%)

[a] The error percentage is given in parentheses as standard error of the mean (SEM)/relative abundance.

peptides. Subtle differences in damage profiles arising from peptides containing internalized and terminal aromatic residues, and from three damage protocols, were resolved sensitively and precisely. This application of isobaric labels confirms that sufficient sensitivity and accuracy may be attained through analysis of individual peptides to provide quantitative information on even low-abundance derivatives.

We envisage that further application of this new approach to damage profiling of residue modifications will permit analogous characterization and tracking of low-abundance residue modifications in a range of complex proteinaceous systems. Isobaric quantitative systems are ideal for more complex systems, as isobaric peptides for quantitative analysis are engineered to coelute. Comparisons of interspecies abundance in more complex systems would naturally have to be limited to species that coelute. In a complex proteomic analysis, the peptides used for protein identification are usually longer than the model peptides utilized in the present study. However, as iTRAQ labeling agents bind to peptides of all sizes as used in proteomic studies, this is not expected to affect the effectiveness of this technique. Notably, relevant potential applications include the utilization of residue-level damage markers to develop and validate protein protective strategies for agricultural products or for tissues such as skin and hair. Tracking may monitor the formation of residue modifications characteristic of specific insults, such as UV exposure, or

may also be utilized to follow the appearance of post-translational modifications induced by cellular means, rather than by exogenous factors. This will allow more sensitive analysis of cell-programmed and damage-induced modification of proteins, yielding more detailed information than is available from cruder, holistic techniques or from nonquantitative MS analysis. Damage profiling offers a route to sensitive evaluation of mitigation strategies developed for protein-based products such as foods and natural textiles or for susceptible cellular tissues.

ABBREVIATIONS USED

TMT, tandem mass tags; IPTL, isobaric peptide termini labeling; UV, ultraviolet; SEM, standard error of the mean; ESI-MS/MS, electrospray ionization−tandem mass spectrometry; Qq-TOF, tandem quadrupole time-of-flight.

LITERATURE CITED

(1) Hains, P. G.; Truscott, R. J. W. Post-translational modifications in the nuclear region of young, aged, and cataract human lenses. *J. Proteome Res*. **2007**, *6*, 3935−3943.

(2) Fu, S.; Davies, M. J.; Stocker, R.; Dean, R. T. Evidence for roles of radicals in protein oxidation in advanced human atherosclerotic plaque. *Biochem. J*. **1998**, *333*, 519−525.

(3) Linton, S.; Davies, M. J.; Dean, R. T. Protein oxidation and ageing. *Exp. Gerontol*. **2001**, *36*, 1503−1518.

(4) Nogueira, A. C. S.; Diceliob, L. E.; Joekes, I. About photodamage of human hair. *Photochem. Photobiol. Sci*. **2006**, *5*, 165−169.

(5) Trautinger, F. Damaged proteins: repair or removal? In *Biophysical and Physiological Effects of Solar Radiation on Human Skin*; Giacomoni, P. U., Ed.; RSC Publishing: Cambridge, U.K., 2007; pp 311−319.

(6) Davidson, R. S. The photodegradation of some naturally occurring polymers. *J. Photochem. Photobiol. B* **1996**, *33*, 3−25.

(7) Leaver, I. H.; Ramsay, G. C. Sensitized photo-oxidation of wool and silk by a triazinylstilbene. *Photochem. Photobiol*. **1969**, *9*, 531−536.

(8) Dalsgaard, T. K.; Otzen, D.; Nielsen, J.; Larsen, L. B. Changes in structures of milk proteins upon photooxidation. *J. Agric. Food Chem*. **2007**, *55*, 10968−10976.

(9) Møller, J. K. S.; Bertelsen, G.; Skibsted, L. H. Photooxidation of nitrosylmyoglobin at low oxygen pressure. Quantum yields and reaction stoechiometries. *Meat Sci*. **2002**, *60*, 421−425.

(10) Osticioli, I.; Nevin, A.; Anglos, D.; Burnstock, A.; Cather, S.; Becucci, M.; Fotakis, C.; Castellucci, E. Micro-Raman and fluorescence spectroscopy for the assessment of the effects of the exposure to light on films of egg white and egg yolk. *J. Raman Spectrosc*. **2008**, *39*, 307−313.

(11) Ronsein, G. E.; de Oliveira, M. C. B.; de Medeiros, M. H. G.; Di Mascio, P. Characterization of O_2 ($^1\Delta_g$)-derived oxidation products of tryptophan: a combination of tandem mass spectrometry analyses and isotopic labeling studies. *J. Am. Soc. Mass Spectrom*. **2009**, *20*, 188−197.

(12) Levine, R. L.; Williams, J. A.; Stadtman, E. P.; Shacter, E.; Lester, P. Carbonyl assays for determination of oxidatively modified proteins. *Methods Enzymol*. **1994**, *233*, 346−357.

(13) Cabiscol, E.; Piulats, E.; Echave, P.; Herrero, E.; Ros, J. Oxidative stress promotes specific protein damage in *Saccharomyces cerevisiae*. *J. Biol. Chem*. **2000**, *275*, 27393−27398.

(14) Shacter, E. Quantification and significance of protein oxidation in biological samples. *Drug Metab. Rev*. **2000**, *32*, 307−326.

(15) Heinecke, J. W.; Li, W.; Daehnke, H. L.; Goldstein, J. A. Dityrosine, a specific marker of oxidation, is synthesized by the myeloperoxidase-hydrogen peroxide system of human neutrophils and macrophages. *J. Biol. Chem*. **1993**, *268*, 4069−4077.

(16) Yuen, C. W. M.; Kan, C. W.; Cheng, S. Y. Evaluation of keratin fibre damages. *Fibers Polym*. **2007**, *8*, 414−420.

(17) Reubsaet, J. L. E.; Beijnen, J. H.; Bult, A.; van Maanen, R. J.; Marchal, J. A. D.; Underberg, W. J. M. Analytical techniques used to study the degradation of proteins and peptides: chemical instability. *J. Pharm. Biomed. Anal*. **1998**, *17*, 955−978.

(18) Halliwell, B.; Whiteman, M. Measuring reactive species and oxidative damage in vivo and in cell culture: how should you do it and what do the results mean? *Br. J. Pharmacol*. **2004**, *142*, 231−255.

(19) Asquith, R. S.; Otterburn, M. S. Self-cross-linking in heated keratin. *J. Text. Inst*. **1970**, *61*, 569−577.

(20) Kerwin, B. A.; Remmele, R. L. J. Protect from light: photodegradation and protein biologics. *J. Pharm. Sci*. **2007**, *96*, 1468−1479.

(21) Criado, S.; Escalada, J. P.; Pajares, A.; García, N. A. Singlet molecular oxygen [$O_2(^1\Delta_g)$]-mediated photodegradation of tyrosine derivatives in the presence of cationic and neutral micellar systems. *Amino Acids* **2008**, *35*, 201−208.

(22) Davies, M. J. The oxidative environment and protein damage. *Biochim. Biophys. Acta − Proteins Proteomics* **2005**, *1703*, 93−109.

(23) Ross, P. L.; Huang, Y. N.; Marchese, J. N.; Williamson, B.; Parker, K.; Hattan, S.; Khainovski, N.; Pillai, S.; Dey, S.; Daniels, S.; Purkayastha, S.; Juhasz, P.; Martin, S.; Bartlet-Jones, M.; He, F.; Jacobson, A.; Pappin, D. J. Multiplexed protein quantitation in *Saccharomyces cerevisiae* using amine-reactive isobaric tagging reagents. *Mol. Cell. Proteomics* **2004**, *3*, 1154−1169.

(24) Aggarwal, K.; Choe, L. H.; Lee, K. H. Quantitative analysis of protein expression using amine-specific isobaric tags in *Escherichia coli* cells expressing *rhsA* elements. *Proteomics* **2005**, *5*, 2297−2308.

(25) Thompson, A.; Schäfer, J.; Kuhn, K.; Kienle, S.; Schwarz, J.; Schmidt, G.; Nuemann, T.; Hamon, C. Tandem mass tags: a novel quantification strategy for comparative analysis of complex protein mixtures by MS/MS. *Anal. Chem*. **2003**, *75*, 1895−1904.

(26) Koehler, C. J.; Strozynski, M.; Kozielski, F.; Treumann, A.; Thiede, B. Isobaric peptide termini labeling for MS/MS-based quantitative proteomics. *J. Proteome Res*. **2009**, *8*, 4333−4341.

(27) Aebersold, R.; Mann, M. Mass spectrometry-based proteomics. *Nature* **2003**, *422*, 198−207.

(28) Aggarwal, K.; Choe, L. H.; Lee, K. H. Shotgun proteomics using the iTRAQ isobaric tags. *Briefings Funct. Genomics Proteomics* **2006**, *5*, 112−120.

(29) Luzchem Technical release: Luzchem exposure standard: LES-UVA-01, http://www.luzchem.com/handbook/LESUVA011.pdf.

(30) Luzchem Technical release: Luzchem exposure standard: LES-UVB-01, http://www.luzchem.com/handbook/LESUVB011.pdf.

(31) Mann, M. Quantitative proteomics? *Nat. Biotechnol*. **1999**, *17*, 954−955.

(32) Lu, Y.; Bottari, P.; Turecek, F.; Aebersold, R.; Gelb, M. H. Absolute quantification of specific proteins in complex mixtures using visible isotope-coded affinity tags. *Anal. Chem*. **2004**, *76*, 4104−4111.

(33) Ehrenshaft, M.; de Oliveira Silva, S.; Perdivara, I.; Bilski, P.; Sik, R. H.; Chignell, C. F.; Tomer, K. B.; Mason, R. P. Immunological detection of *N*-formylkynurenine in oxidized proteins. *Free Radical Biol. Med*. **2009**, *46*, 1260−1266.

(34) Grosvenor, A. J.; Morton, J. D.; Dyer, J. M. Profiling of residue-level photo-oxidative damage in peptides. *Amino Acids* **2010**, *39*, 285−296.

(35) Dyer, J. M.; Bringans, S. D.; Bryson, W. G. Determination of photo-oxidation products within photoyellowed bleached wool proteins. *Photochem. Photobiol*. **2006**, *82*, 551−557.

(36) Igarashi, N.; Onoue, S.; Tsuda, Y. Photoreactivity of amino acids: tryptophan-induced photochemical events *via* reactive oxygen species generation. *Anal. Sci*. **2007**, *23*, 943−948.

(37) Davies, M. J. Singlet oxygen-mediated damage to proteins and its consequences. *Biochem. Biophys. Res. Commun*. **2003**, *305*, 761−770.

(38) Broo, K. S.; Brive, L.; Sott, R. S.; Baltzer, L. Site-selective control of the reactivity of surface-exposed histidine residues in designed four-helix-bundle catalysts. *Folding Design* **1998**, *3*, 303−312.

(39) Bruskov, V. I.; Malakhova, L. V.; Masalimov, Z. K.; Chernikov, A. V. Heat-induced formation of reactive oxygen species and 8-oxoguanine, a biomarker of damage to DNA. *Nucelic Acids Res*. **2002**, *30*, 1354−1363.

Received for review August 25, 2010. Revised manuscript received November 3, 2010. Accepted November 8, 2010. Funding for this project was provided through a Wool Research Organisation of New Zealand Inc. and New Zealand Wool Industry Charitable Trust Post-Graduate Scholarship and through the New Zealand Foundation for Research, Science and Technology.